A One-Pot Synthesis of 1,3-Dihydro-1,3,3-tris(perfluoroalkyl)isobenzofuran-1-olates and Their Complete NMR Spectroscopic Analysis on the Basis of 1D and 2D Experiments

by **Wieland Tyrra***[a]), **Harald Scherer**[a]), **Lesya A. Babadzhanova**[b]), **Natalya V. Kirij**[b]), **Yurii L. Yagupolskii**[b]), **Dieter Naumann***[a]), and **Ingo Pantenburg**[a])

[a]) Institut für Anorganische Chemie, Universität zu Köln, Greinstrasse 6, D-50939 Köln (fax: +49-221-470-5196; e-mail: tyrra@uni-koeln.de; d.naumann@uni-koeln.de)

[b]) Institute of Organic Chemistry, National Academy of Sciences of Ukraine, Murmanskaya-5, UA-02094 Kiev, Ukraine

A convenient synthesis of the 1,3-dihydro-1,3,3-tris(perfluoroalkyl)isobenzofuran-1-ols **3a**,**b** was elaborated starting from commercially available phthaloyl dichloride and trimethyl(perfluoroalkyl)silanes (Me_3SiR_f) **1a**,**b** ($R_f = CF_3$, C_2F_5) in the presence of a fluoride source (*Schemes 1* and *3*). In a reaction analogous to alkyl *Grignard* reagents, double chloride substitution by two perfluoroalkyl groups and subsequent addition of one perfluoroalkyl group with concomitant ring closure led to this new class of compounds (*Scheme 2*). The syntheses of the alcohols and some alcoholates, as well as of the corresponding trimethylsilyl ethers are described. A combination of special 1D and 2D NMR experiments allowed the assignment of all atoms of the new compounds. The solid-state structure of 1,3-dihydro-1,3,3-tris(trifluoromethyl)isobenzofuran-1-ol (**3a**) was elucidated by X-ray diffraction methods.

1. Introduction. – Trimethyl(perfluoroalkyl)silanes are widely used in different reactions in organic and element organic synthesis [1]. The diversity of these reactions spreads from additions to hetero-multiple bonds to nucleophilic substitutions. (Perfluoroalkyl)silicates [2] intermediately formed in solution turned out as those reagents of high nucleophilicity which prevent a selective conversion of acid chlorides into the corresponding perfluoroalkyl ketones [3] but allow a selective synthesis of 2-alkyl- or 2-aryl-1,1,1,3,3,3-hexafluoropropan-2-ols [4].

On the other hand, already in the early 1970s, 1,3,3-trialkylated 1,3-dihydroisobenzofuranols attracted some attention as building blocks for 1-vinyl-1-phthalanpropylamines which were suggested as potential antidepressant agents [5]. The general method for their synthesis – best elaborated for the fully methylated derivative is treatment of phthalic esters with methylmagnesium halides – had been established some years earlier [6]. Due to the unavailability of (trifluoromethyl)magnesium halides, some related trifluoromethyl derivatives have been prepared starting from 1,2-dibromobenzene *via* sequential lithium–halogen exchange and treatment of the organolithium derivatives with trifluoroacetic acid methyl ester. This reaction sequence opened an access to 1-(trifluoromethyl)- [7] and 1,3-bis(trifluoromethyl)-substituted [8] 1,3-dihydroisobenzofuran-1-ols. Also 1,3-dihydro-1-(trifluoromethyl)isobenzofuran-1-ols are expected to be esterase and protease inhibitors [7]; therefore, the

furanols described in this paper may be suggested as new versatile building blocks either for pharmaceuticals [5][7] or for weakly coordinating anions [9] because they can formally be seen as space-demanding alcohols with electron-withdrawing substituents.

The ^{1}H-, ^{13}C-, and ^{19}F-NMR data of some 1,3-dihydroisobenzofuran-1-ols have been compiled [7][8][10], but no systematic approach has been made for a complete assignment although for an understanding of the complex spin systems of some of those derivatives and especially for the newly generated 1,3,3-tris(perfluoroalkyl) compounds, a complete analysis is essential.

2. Results and Discussion. – 2.1. *Synthesis of* **2** *and Conversions to* **3**, **4**, *and* **5**. In continuation of our previous work [4], we investigated the reactions of phthaloyl dichloride and trimethyl(perfluoroalkyl)silanes (Me_3SiR_f) **1a** ($R_f = CF_3$) and **1b** ($R_f = C_2F_5$) in the presence of a fluoride source which yielded **2a**,**b** (*Scheme 1*). The reactions were performed in 1,2-dimethoxyethane (= glyme) between $-60°$ and room temperature with Me_4NF, CsF, and [Cs(15-crown-5)$_2$]F as fluoride sources. Best results were obtained with Me_4NF, Me_3SiR_f, and phthaloyl dichloride in a molar ratio of 3:3:1 (*Scheme 1*). It must be noted that even if a 25% excess of Me_3SiCF_3 (**1a**) was used, no evidence for products due to the reaction of **1a** with itself was found [11]. CF_3H and C_2F_5H were detected as the dominant by-products in the ^{19}F-NMR spectra of the reaction mixtures.

Scheme 1

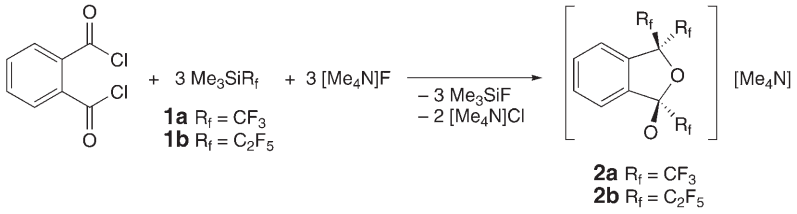

Directly after the addition of Me_4NF to a mixture of phthaloyl dichloride and the corresponding silane **1** at $-60°$, the reaction mixture became turbid indicating the rapid formation of Me_4NCl. After *ca.* 1 h of stirring at $-50°$, pale-yellow, milky suspensions were obtained suggesting that the conversion of the dichloride into the corresponding intermediately formed diketones was completed. ^{19}F-NMR Spectra recorded (only for reactions with **1a**) at $-40°$ after a reaction time of 30 min showed exclusively intensive *s* in the region between δ -70 and -74 which should be attributed to (trifluoromethyl) keton functions in comparison with literature data [12][13]. This, together with the observation that directly after addition of Me_4NF, a white solid was formed, implies chloride substitution being the first step in the formation of compounds **2** (*Scheme 2*). Upon attack of the third perfluoroalkyl nucleophile, the proximity of the two carbonyl functions leads to the formation of the cyclic ethers *via* internal nucleophilic attack of the initial intermediate at the adjacent carbonyl C-atom in a similar manner as outlined by *Tamborski et al.* for reactions of

1,2-bis(trifluoroacetyl)benzene (=1,1′-(1,2-phenylene)bis[2,2,2-trifluoroethanone]) with several O- and N-nucleophiles [8][14].

Scheme 2

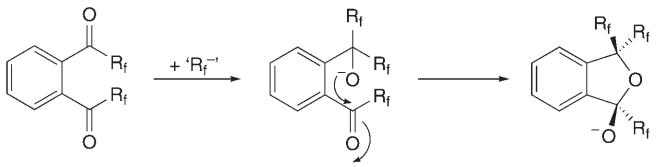

Manipulations to obtain the alcohols **3** (*Scheme 3*), the silanes **4** (*Scheme 4*), as well as the stannane **6a**, and the cation exchange to obtain salts **5** (*Scheme 4*) with the bulky $(Ph_3P=)_2N^+$ cation may be seen as standard procedures making use of the generally very low solubility of the heavier tetramethylammonium halides in common organic solvents.

Scheme 3

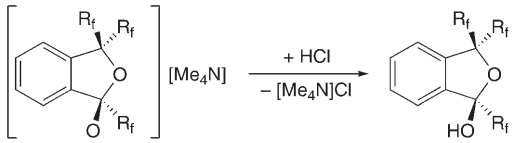

2a $R_f = CF_3$
2b $R_f = C_2F_5$

3a $R_f = CF_3$
3b $R_f = C_2F_5$

2.2. *NMR Analysis of* **6a**. The assignment of the NMR resonances was achieved by a combination of $^{13}C,^1H$, $^{13}C,^{19}F$, $^{19}F,^1H$, and $^{19}F,^{19}F$ correlation experiments as well as by $^{19}F,^1H$- and $^{19}F,^{19}F$-NOE spectra (*Tables 1* and *2*). The proceeding of the NMR analysis is discussed exemplary for **6a** (for the (arbitrary) atom numbering, *cf.* **5a** in *Scheme 4*).

In the ^1H-decoupled $^{13}C,^{19}F$-HMBC spectrum of **6a** *(Fig. 1)*, the signals of the quaternary sp^3 C-atoms in the five-membered ring are detected at δ 85.5 (C(3)) and 111.4 (C(1)) by correlation with the F-resonances of the CF_3 groups *via* $^2J(C,F)$ coupling constants. Furthermore, the resonance at δ 85.5 correlates to two F-signals at δ −75.6 ($^2J(C,F) = 28$ Hz) and −75.7 ($^2J(C,F) = 32$ Hz), whereas the signal at δ 111.4 shows only one cross-peak to the F-resonance at δ −82.0 ($^2J(C,F) = 34$ Hz). This correlation offers concomitant identification of the positions of these C-atoms and the CF_3 groups. The assignment of the δ(C) of the CF_3 groups is achieved by careful interpretation of the cross-peaks caused by $^1J(C,F)$ couplings which all three show the typical absolute value of *ca.* 288 Hz for CF_3 groups bond to sp^3-hybridized C-atoms.

The orientation of the CF_3 groups in **6a** was studied by $^{19}F,^1H$-NOE spectra. In the $^{19}F,^1H$-HOESY plot (*Fig. 2*) the proton signal of the Me_3Sn group is easily identified by its highfield chemical shift of δ 0.44 and its Sn satellites. This resonance shows NOE cross-peaks to the F-signal at δ −82.0 of the CF_3 group (C(10)) attached to the same C-atom and to the F-signal at δ −75.6. Therefore, the latter CF_3 group (C(11)) must be directed to the same ring side as the Me_3Sn group.

Scheme 4

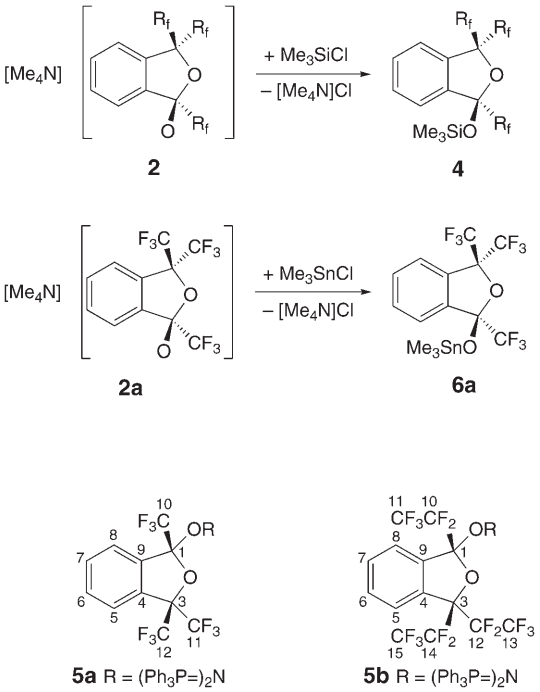

Table 1. *^{13}C-NMR Data* (100.61 or 75.47 MHz) *of Compounds* **3a**–**6a** *in CD_3CN* (**2a**/**5a** and **6a**) *and $CDCl_3$* (**3a** and **4a**). δ in ppm, J in Hz. For the arbitrary atom numbering, see **5a** in *Scheme 4*.

	2a/5a[a])	**3a**	**4a**	**6a**
C(1)	126.3	106.6	107.2	111.4
C(3)	81.7	86.9	87.0	85.5
C(4)	133.4	131.4	130.8	130.6
C(5)	123.4	123.7	123.5	123.6
C(6)	128.4	132.0	131.2	131.1
C(7)	130.3	132.2	131.9	132.3
C(8)	123.9	124.2	123.9	123.9
C(9)	145.2	136.5	138.5	140.4
C(10)	123.7	121.64	121.7	122.8
C(11)	123.4	121.4	121.7	122.2
C(12)	123.6	121.56	121.5	122.1
C(13)	–	–	0.8 (^1J(C,^{29}Si) = 60.4)	– 1.5 (^1J(C,^{119}Sn) = 430)

[a]) Shifts are extremely dependent on concentration.

Additionally, NOEs of all three CF_3 groups of **6a** to aromatic protons are found. Since the *ABCD* spin system of the aromatic protons shows strong high-order effects, an easy interpretation of the splitting patterns is impossible. The NOE information

Table 2. *^{1}H- and ^{19}F-NMR Data* (400.13 or 300.13 and 376.4 or 282.4 MHz, resp.) *of Compounds* **3a**–**6a** *in CD_3CN* (**2a**/**5a** and **6a**) *and $CDCl_3$* (**3a** and **4a**). δ in ppm, J in Hz. For the arbitrary atom numbering, see **5a** in *Scheme 4*.

	2a/5a[a]) (c = 0.10/0.11M)		**3a** (c = 0.29M)		**4a** (c = 0.24M)		**6a** (c = 0.20M)	
	δ(H)[b])	δ(F)	δ(H)[b])	δ(F)	δ(H)[b])	δ(F)	δ(H)[b])	δ (F)
H–C(5)	7.44		7.59		7.64		7.62	
H–C(6)	7.41		7.61		7.64		7.64	
H–C(7)	7.46		7.63		7.62		7.67	
H–C(8)	7.38		7.63		7.62		7.56	
CF_3(10)		−80.9 (*q*, ^6J(F,F) = 6.6)		−82.7 (*q*, ^6J(F,F) = 5.6)		−81.1 (*q*, ^6J(F,F) = 5.9)		−82.0 (*q*, ^6J(F,F) = 6.2)
CF_3(11)		−76.1 (*q*, ^4J(F,F) = 10.0)		−75.2 (*q*, ^4J(F,F) = 9.7)		−75.0 (*q*, ^4J(F,F) = 10.0)		−75.6 (*q*, ^4J(F,F) = 9.7)
CF_3(12)		−75.4 (*m*)		−75.8 (*m*)		−75.1 (*m*)		−75.7 (*m*)
$Me(13)_3$					0.26 (*s*, ^2J(^{29}Si,H) = 6.8)[c])		0.44 (*s*, ^2J(^{119}Sn,H) = 65.0)[d])	
OH			5.0 (br.)					

[a]) Shifts are extremely dependent on concentration. [b]) *ABCD* Spin system displaying strong effects of higher order. [c]) δ(^{29}Si) 22.2. [d]) δ(^{119}Sn) 112.4.

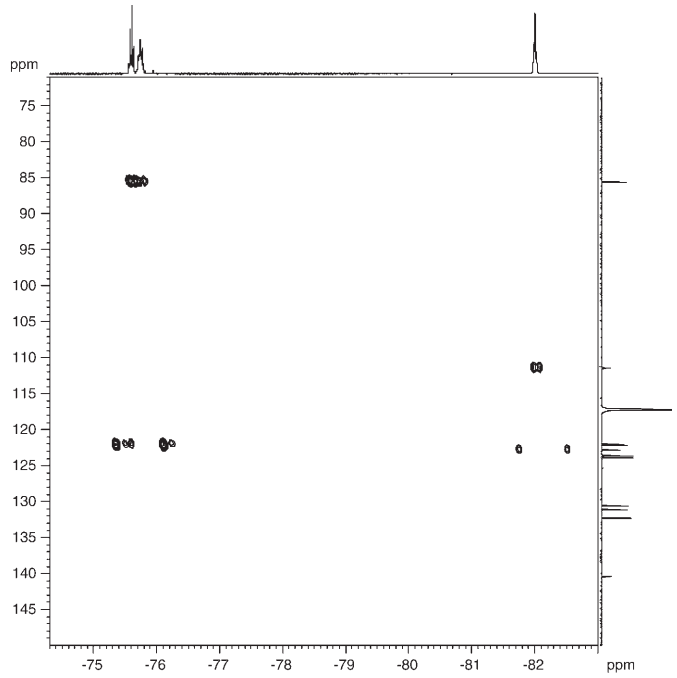

Fig. 1. *$^{13}C,^{19}F$-HMBC Spectrum* (CD_3CN; ^1H-decoupled) *of* **6a**, *optimized for coupling constants of 30 Hz*

offers the best approach to the analysis of the benzene ring. Hence, the proton signal at δ 7.56 (H–C(8)) must be assigned to a proton in the neighborhood of the CF_3 group with the F-signal at δ −82.0 (C(10)). Consequently, due to the NOEs of the CF_3 groups at δ −75.6 (C(11)) and −75.7 (C(12)), the proton signal at δ 7.62 has to be assigned to H–C(5).

By means of ^1J(C,H) correlation spectroscopy, the corresponding C-resonances are found at δ 123.9 (C(8)) for the proton signal at δ 7.56 (H–C(8)), and at δ 123.6 (C(5)) for the proton signal at δ 7.62 (H–C(5)). The remaining proton resonances correlate as follows: δ(H) 7.67/δ(C) 132.3 (C(7)), δ(H) 7.64/δ(C) 131.1 (C(6)), δ(H) 0.44/δ(C) −1.5 (Me_3Sn).

The final assignment of the resonances of the benzene ring was achieved by a ^{19}F-decoupled $^{13}C,^1H$-HMBC spectrum, taking into account that ^3J(C,H) coupling constants are generally greater than ^2J(C,H) coupling constants in benzene rings. On the other hand, electron-withdrawing substituents increase the absolute values of ^2J(C,H) coupling constants making the occurrence of these cross-peaks very likely. Additional cross-peaks due to ^4J(C,H) couplings are found.

The signal of H–C(5) at δ 7.62 shows its major long-range cross-peak to the C-resonance at δ 132.3 which is assigned to C(7) (*Fig. 3*). Moreover, the cross-peak of this proton resonance to the signal of the quaternary sp^2 C-atom at δ 140.4 is significantly more intensive than the corresponding cross-peak of H–C(8) at δ 7.56. As a consequence, the resonance at δ 140.4 is the signal of C(9). Finally, the C-signals at

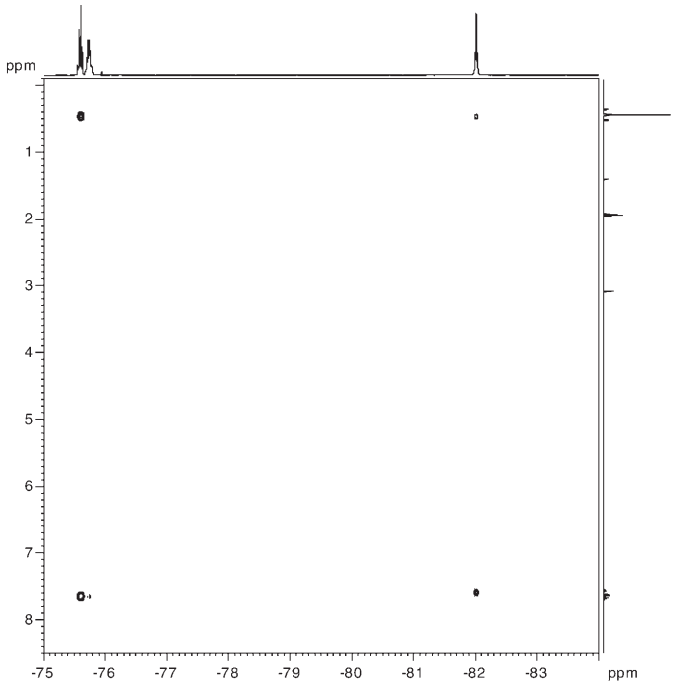

Fig. 2. *$^{19}F,^{1}H$-HOESY Plot* (CD_3CN) *of* **6a**

130.6 and 131.1 are found to be the resonances of C(4) and C(6) which is supported by the long-range cross-peaks of H–C(8). The ^{3}J(C,H) cross-peaks of H–C(8) to the signal of C(1) at δ 111.4 and of H–C(5) to the resonance of C(3) at δ 85.5 support the information obtained from the $^{19}F,^{1}H$-NOE spectrum.

All other compounds derived from the 1,3-dihydro-1,3,3-tris(trifluoromethyl)isobenzofuran-1-ol (**3a**) were analyzed in a similar manner as **6a**. The results are compiled in *Tables 1* and *2*. As general tendencies, the δ(C) of C(1) in the **a** series is always detected downfield from the signal of C(3), the δ(C) of C(9) always downfield from that of C(4), and the signal of C(1) is shifted to lower field with increasing negative polarization by the O-containing moiety. The δ(F) of CF_3(10) is significantly shifted to highfield as compared to the signals of the other CF_3 groups (δ(F) *ca.* -76), by *ca.* 5 ppm (δ(F) < -80 ppm). It is noteworthy that the signal of C(10) is split into a *q* by a formal ^{6}J(F,F) coupling of 5–6 Hz to one of the other CF_3 groups. In the $^{19}F,^{19}F$-COSY plot of **6a** (*Fig. 4*), its coupling partner is identified to be CF_3(12). As it was found from the $^{19}F,^{1}H$-NOE plot (*Fig. 2*), CF_3(12) points to the same ring side as CF_3(10). The ^{19}F-1D-NOE NMR (^{19}F-DPFGSENOE) spectrum (*Fig. 5*) demonstrates that the spacial distance is short enough to give rise to a $^{19}F,^{19}F$-NOE. Such a through-space interaction contributes significantly to the large coupling constant between these CF_3 groups. This proposal is supported by the shortest F···F distance of 290 pm of those CF_3 groups found in the molecular structure of **3a** (*cf. 2.3*). In future investigations, this significant coupling will simplify the determination of the orientation of the CF_3 groups by mere

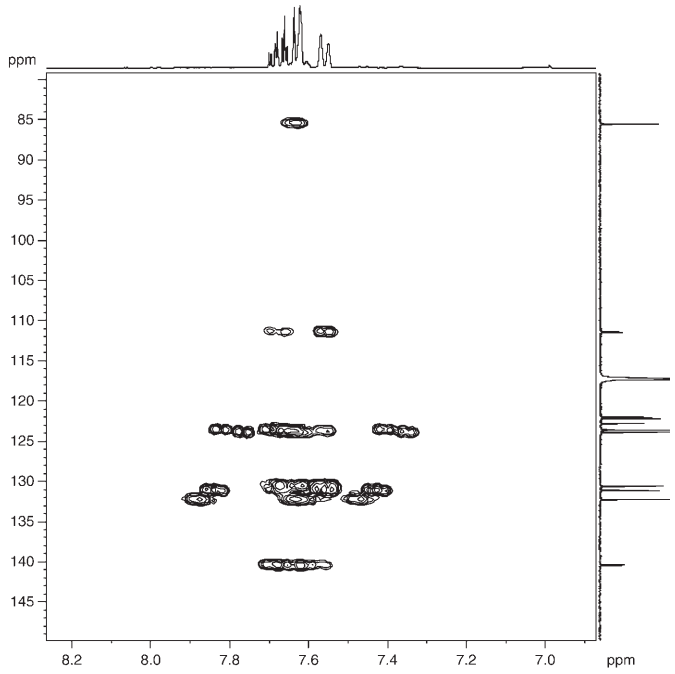

Fig. 3. *Section of the aromatic signals in the $^{13}C,^{1}H$-HMBC spectrum* (CD_3CN) *of* **6a**, *optimized for coupling constants of 7 Hz*

interpretation of the splitting pattern of the F-signals of the CF_3 groups or by a $^{19}F,^{19}F$-COSY experiment.

The NMR analyses of the 1,3-dihydro-1,3,3-tris(pentafluoroethyl)isobenzofuran-1-ol derivatives **2b**–**5b** were performed in a similar manner. An additional complication arises from the fact that the F-atoms of the CF_2 groups are not chemically equivalent. The knowledge about the chemical shifts of the ring C-atoms together with the intensive investigations on the CF_3 derivatives of the **a** series turned out to be very helpful for the final assignment. The results are summarized in *Table 3*. A complete NMR analysis of **4b** became impossible because the molecule underwent fast hydrolysis in solution. It should be noted that also for the molecules of the **b** series, some exceptionally large F,F-couplings are observed between selected F-resonances. In the ^{19}F-NMR spectrum of **3b**, *e.g.*, a J(F,F) of 26.8 Hz is observed between the F-signals at δ −116.3 (CF_2(14)) and −122.5 (CF_2(10)).

2.3. *Solid-State Structure of 1,3-Dihydro-1,3,3-tris(trifluoromethyl)isobenzofuran-1-ol* (**3a**). Compound **3a** crystallizes in the tetragonal space group $P4_2/n$ (no. 86) with 8 molecules per unit cell. Its bond length and angles do not exhibit any peculiarities in comparison with related structures [8]. The molecule is quasi-planar with the ring O-atom deviating marginally from absolute planarity opposite to the OH group (*Fig. 6*). The H-atom of the OH group was included as individual atom with free positional and isotropic displacement parameters. Four molecules of **3a** generate a closed ring by way of four O(3)–H(5)$\cdots$O(3′) bonds (*Fig. 7*), thus characterized by an R_4^4 (8) motif [15].

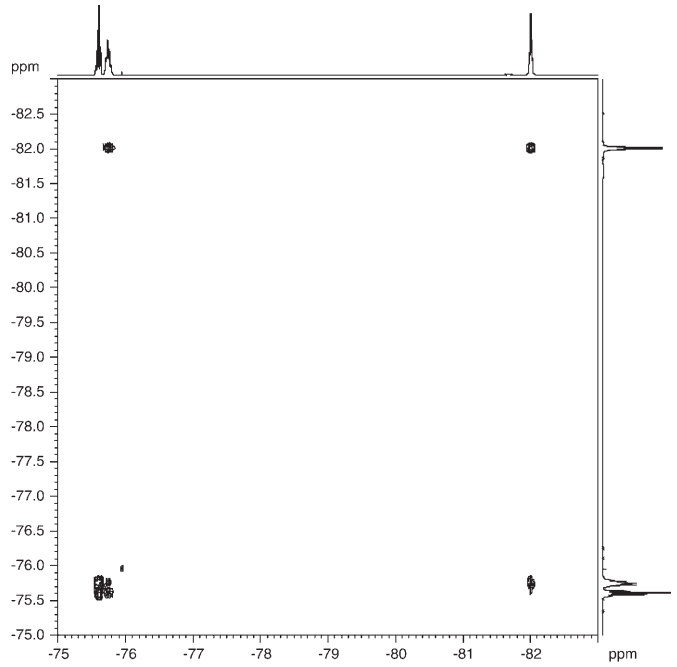

Fig. 4. *^{19}F,^{19}F-COSY Plot* (CD_3CN) *of* **6a**

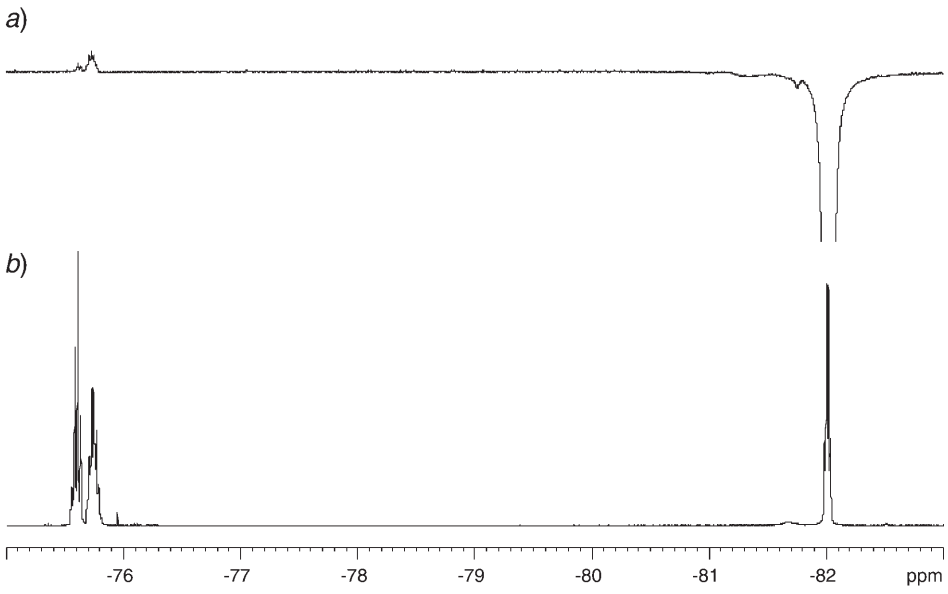

Fig. 5. a) *^{19}F-1D-NOE NMR Spectrum* (CD_3CN; selective excitation at δ −82) *and* b) ^{19}F-NMR spectrum (CD_3CN) *of* **6a**

Table 3. *NMR Data* (400.13, 376.4, or 100.61 MHz, CD_3CN) *for Compounds* **2b**–**4b**. δ in ppm, J in Hz. For the arbitrary atom numbering, see **5b** in *Scheme 4*.

	2b[a]) ($c = 0.18$M)			**3b** ($c = 0.20$M)			**4b** ($c = 0.18$M)
	δ(C)	δ(H)[b])	δ(F)	δ(C)	δ(H)[b])	δ(F)	δ(F)
C(1)	125.1			108.9			
C(3)	84.2			89.2			
C(4)	134.9			130.9			
H–C(5)	124.5	7.51		124.8	7.77		
H–C(6)	128.2	7.41		132.2	7.80		
H–C(7)	130.0	7.46		132.2	7.80		
H–C(8)	124.6	7.44		124.8	7.81		
C(9)	144.7			135.8			
CF_2(10)	112.3		−118.3, −119.4 (br., ^2J(F,F) = 266)	111.2		−122.5, −122.8 (2*m*, ^2J(F,F) = 275)	−121.5, −123.1 (2*m*, ^2J(F,F) = 275)
CF_3(11)	120.2		−78.5 (*m*)	118.7		−79.7 (*m*)	−79.4 (*m*)
CF_2(12)	114.0		−115.8, −118.4 (br., ^2J(F,F) = 282)	112.1		−116.0, −117.2 (2*m*, ^2J(F,F) = 291)	−113.6, −115.9 (2*m*, ^2J(F,F) = 291)
CF_3(13)	118.8		−78.5 (br.)	118.2		−79.6 (*m*)	−79.7 (*m*)
CF_2(14)	114.0		−114.3, −116.5 (br., ^2J(F,F) = 289)	112.1		−116.3, −117.3 (2*m*, ^2J(F,F) = 295)	−116.3, −117.3 (2*m*, ^2J(F,F) = 295)
CF_3(15)	118.9		−78.9 (br.)	118.2		−79.2 (*m*)	−79.1 (*m*)
OH					6.51 (*d*, ^4J(F,H) = 1.8)		

[a]) Shifts are extremely dependent of concentration. [b]) *ABCD* Spin system displaying strong effects of higher order.

All contacts fall into the range of characteristic O–H···O bridges with the H-bonding geometry *D*–H 0.80(3) Å, H···*A* 2.07(3) Å, *D*···*A* 2.827(2) Å, *D*–H···*A* 156(3)°. A view along the crystallographic *c*-axis (*Fig. 8*) shows this $R_4^4(8)$ motif within the crystal structure. F-Channels are oriented parallel to the crystallographic *a*-axis.

Generous financial support of this work by the *Deutsche Forschungsgemeinschaft* is gratefully acknowledged (436 UKR 113/26). We are indebted to Dr. *Mathias Schäfer* (Institut für Organische Chemie, Universität zu Köln) (ESI-MS), *Astrid Baum* (EI-MS), *Daniela Naumann* (NMR), *Nurgül Tosun* (elemental analysis), and *Silke Kremer* (materials, EI-MS, elemental analysis).

Experimental Part

General. All reactions were carried under dry Ar or N_2 by using *Schlenk* techniques. Me_3SiCF_3 was purchased from *ABCR* and phthaloyl dichloride from *Acros*. $Me_3SiC_2F_5$ was prepared from C_2F_5I, Me_3SiCl, and $P(NEt_2)_3$ following the *Ruppert* procedure [16], Me_4NF from $Me_4N(BF_4)$ and KF [17], and bis(triphenylphosphoranylidene)ammonium iodide ($(Ph_3P{=})_2NI$) from the chloride by halide exchange with NaI [18]. With the exception of glyme (=1,2-dimethoxyethane; *Aldrich*), all solvents and reagents were purified according to literature procedures [19]. The {[1,3-dihydro-1,3,3-tris(trifluoromethyl)isobenzofuran-1-yl]oxy}trimethylstannane (**6a**) was prepared only for NMR investigations following the procedure for **4** but was not further characterized. M.p.: *Stuart SMP-10* apparatus; one-end-open glass capillaries; uncorrected. NMR Spectra: *Bruker Avance-II-300* or *Avance-400* spectrometer; *Avance-II-300: ATM BBFO* probehead, detection coil tuned to the frequency of ^{13}C of 75.47 MHz (90° pulse:

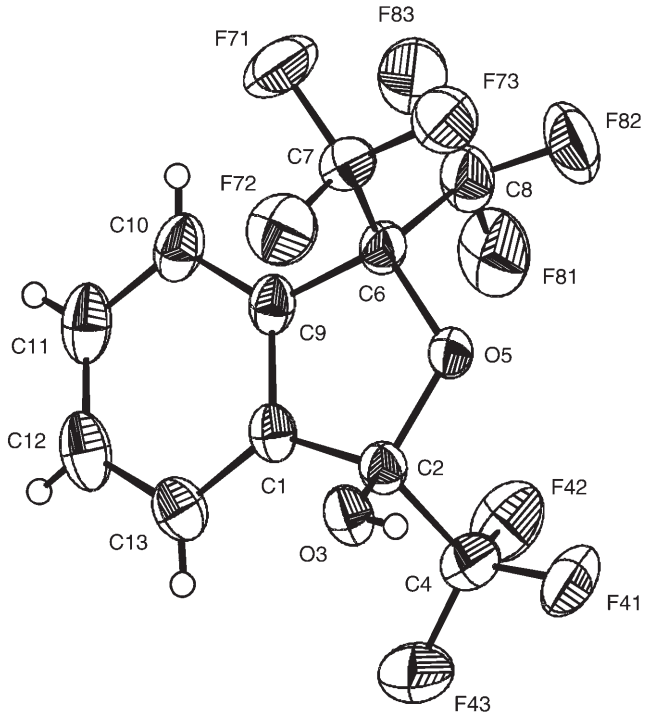

Fig. 6. *Molecular structure of* **3a**. Thermal ellipsoids (except for H) are drawn at the 50% probability level; selected bond lengths [Å] and angles [°] (with estimated standard deviations in parentheses): C(2)–O(5) 1.427(2), O(5)–C(6) 1.427(2), C(6)–C(9) 1.507(3), C(1)–C(9) 1.375(3), C(1)–C(2) 1.501(3), C(6)–C(7) 1.530(4), C(6)–C(8) 1.531(3), C(2)–C(4) 1.530(3), C(2)–O(3) 1.394(2), C(9)–C(1)–C(2) 109.7(2), C(1)–C(2)–O(5) 104.7(2), C(7)–C(6)–C(8) 112.0(2), C(4)–C(2)–O(5) 109.3(2), C(2)–O(5)–C(6) 111.4(2), O(5)–C(6)–C(9) 105.2(2), C(6)–C(9)–C(1) 108.4(2).

10.6 μs) or ^{29}Si of 59.63 MHz (90° pulse: 10.5 μs), decoupler coil tuned to the frequency of either ^{1}H (300.13 MHz; 90° pulse: 11.7 μs) or ^{19}F (282.4 MHz; 90° pulse: 13.5 μs); *Avance-400:* triple-resonance ^{1}H,^{19}F,*BB TXI*-probehead; broad-band coil tuned to the frequency of ^{13}C of 100.61 MHz (90° pulse: 12 μs) or of ^{119}Sn of 149.21 MHz (90° pulse: 9 μs), detection coil simultaneously tuned to the ^{1}H frequency of 400.13 MHz (90° pulse: 11.5 μs), and the ^{19}F frequency of 376.4 MHz (90° pulse: 13 μs); chemical shifts rel. to $SiMe_4$ (^{1}H,^{13}C,^{29}Si), CCl_3F (^{19}F), and Me_4Sn (^{119}Sn), respectively. MS: *Finnigan MAT 95* (20 eV) for EI and *Finnigan MAT 900* for ESI (MeCN, flow rate 2 μl/min); in *m*/*z* (rel. %). Elemental analyses: *HEKAtech Euro EA 3000.*

Tetramethylammonium 1,3-Dihydro-1,3,3-tris(trifluoromethyl)isobenzofuran-1-olate (**2a**). To a well-stirred mixture of phthaloyl dichloride (2.60 g, 12.8 mmol) in anh. glyme (50 ml), Me_3SiCF_3 (**1a**; 6.00 g, 42.3 mmol) and Me_4NF (3.60 g, 38.7 mmol) were added at −60°. Stirring was maintained for 1 h at −50° and for additional 24 h at r.t. The formed Me_4NCl was filtered off, and all volatile materials were condensed *in vacuo* at r.t.: 4.49 g (85%) of crude **2a**, contaminated by up to 5% of Me_4NCl. Attempted further purification by crystallization unfortunately failed. Colorless solid. ESI-MS (neg.): 339.2 (100, M^-).

Tetramethylammonium 1,3-Dihydro-1,3,3-tris(1,1,2,2,2-pentafluoroethyl)isobenzofuran-1-olate (**2b**). As described for **2a**, from phthaloyl dichloride (0.76 g, 3.8 mmol), $Me_3SiC_2F_5$ (**1b**; 2.37 g, 12.3 mmol), Me_4NF (1.00 g, 10.7 mmol), and glyme (15 ml). Recrystallization from Et_2O/hexane 1:1 (*v*/*v*) yielded

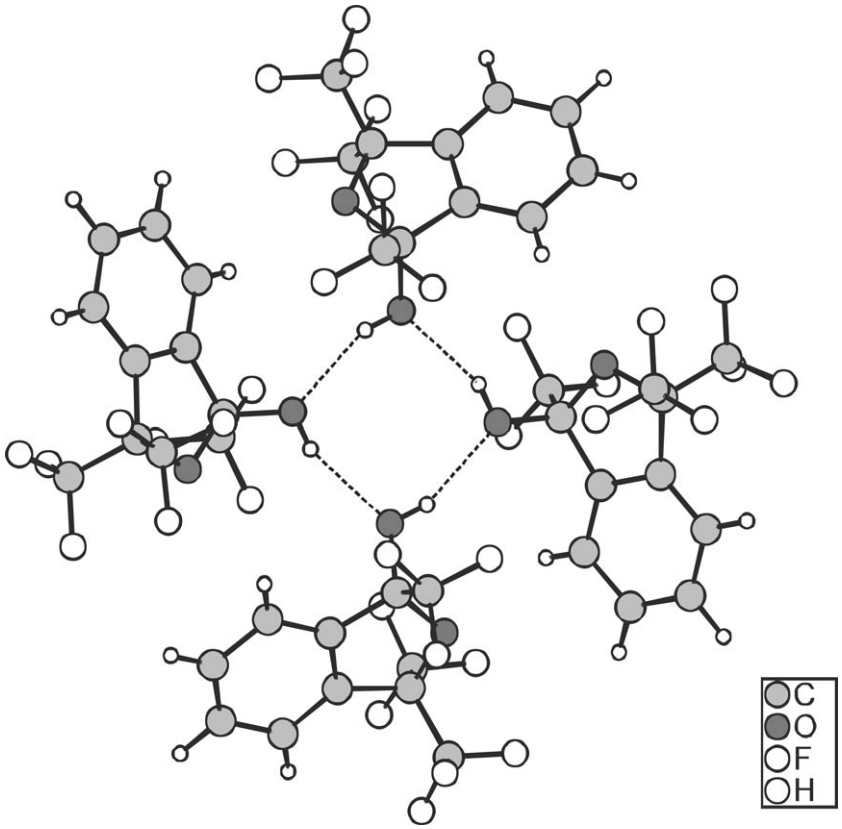

Fig. 7. *View of a tetrameric unit of* **3a**

1.31 g (62%) of **2b**. Colorless solid. M.p. 83–85° (dec.). ESI-MS (neg.): 489.2 (100, M^-). Anal. calc. for $C_{18}H_{15}F_{15}NO_2$ (563.30): C 38.38, H 2.86, N 2.49; found: C 37.41, H 3.02, N 2.55.

1,3-Dihydro-1,3,3-tris(trifluoromethyl)isobenzofuran-1-ol (**3a**) *and 1,3-Dihydro-1,3,3-tris(1,1,2,2,2-pentafluoroethyl)isobenzofuran-1-ol* (**3b**). To a suspension of **2a** or **2b** (2 mmol) in Et_2O (10 ml), 3N HCl (15 ml) was added. After stirring for 15 min, the aq. phase was extracted twice with Et_2O (10 ml). The combined org. phase was washed with H_2O (10 ml), dried ($MgSO_4$), and concentrated, and the residue purified by vacuum sublimation (**3a**) or vacuum distillation (**3b**).

Data of **3a**: Yield 70.6% (0.48 g). Colorless solid. M.p. 69–70° (dec.). EI-MS: 271 (100, $[M-CF_3]^+$). Anal. calc. for $C_{11}H_5F_9O_2$ (340.2): C 38.83, H 1.48; found: C 38.96, H 1.54.

Data of **3b**: Yield 67.0% (0.75 g). Colorless liquid. B.p. 52–53° ($1.2\cdot10^{-2}$ mbar). EI-MS: 371 (100, $[M-C_2F_5]^+$), 252 (15, $[M-2\,C_2F_5]^+$). Anal. calc. for $C_{14}H_5F_{15}O_2$ (490.2): C 34.30, H 1.03; found: C 34.47, H 1.09.

{[1,3-Dihydro-1,3,3-tris(trifluoromethyl)isobenzofuran-1-yl]oxy}trimethylsilane (**4a**) *and {[1,3-Dihydro-1,3,3-tris(1,1,2,2,2-pentafluoroethyl)isobenzofuran-1-yl]oxy}trimethylsilane* (**4b**). To a suspension of **2a** or **2b** (2 mmol) in Et_2O (20 ml), Me_3SiCl (0.27 g, 2.50 mmol) was added. The mixture was stirred for 1 h at r.t. The formed precipitate (Me_4NCl) was filtrated, and the solvent and excess Me_3SiCl were evaporated. The product **4a** or **4b** was extracted with pentane and purified by column chromatography (silica gel, pentane).

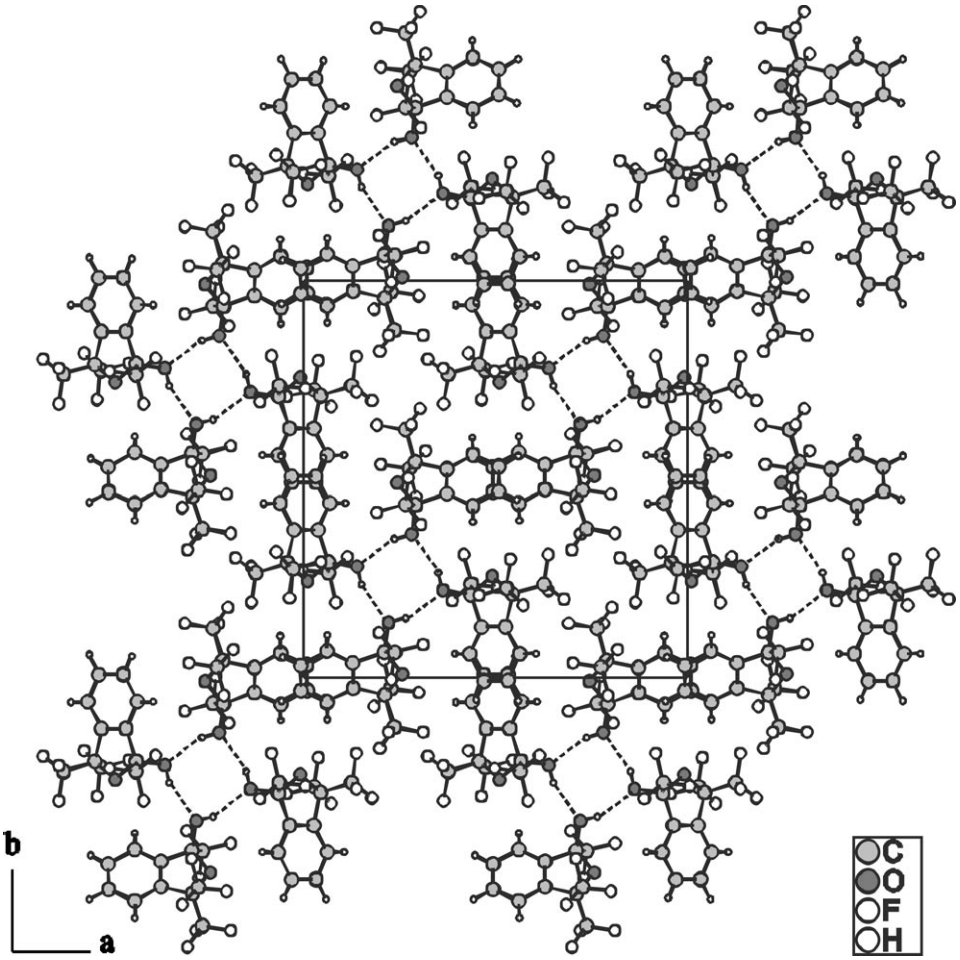

Fig. 8. *The packing diagram of* **3a** *viewed along the crystallographic* c*-axis*

Data of **4a**: Yield 78% (0.64 g). Colorless oil. EI-MS: 397 (100, $[M-Me]^+$). Anal. calc. for $C_{14}H_{13}F_9O_2Si$ (412.3): C 40.79, H 3.18; found: C 40.64, H 3.11.

Data of **4b**: Yield 72% (0.81 g). EI-MS: 547 (100, $[M-Me]^+$), 473 (15, $[M-OSiMe_3]^+$). Anal. calc. for $C_{17}H_{13}F_{15}O_2Si$ (562.3): C 36.21, H 2.33; found: C 36.43, H 2.39.

Bis(triphenylphosphoranylidene)ammonium 1,3-Dihydro-1,3,3-tris(trifluoromethyl)isobenzofuran-1-olate (**5a**) *and Bis(triphenylphosphoranylidene)ammonium 1,3-Dihydro-1,3,3-tris(1,1,2,2,2-pentafluoroethyl)isobenzofuran-1-olate* (**5b**). To a soln. of **2a** or **2b** in CH_2Cl_2 (10 ml), $(Ph_3P{=})_2NI$ (0.66 g, 1.0 mmol) was added. The mixture was stirred for 1 h at r.t., while white Me_4NI precipitated which was filtered off. The solvent was evaporated giving the salt **5a** or **5b**.

Data of **5a**: Yield 95% (0.83 g). Colorless solid. M.p. 208–210° (dec.). Anal. calc. for $C_{47}H_{34}F_9NO_2P_2$ (877.8): C 64.30, H 3.90, N 1.60; found: C 63.57, H 3.99, N 1.67.

Data of **5b**: Yield 87% (0.90 g). Colorless solid. M.p. 86–87° (dec.). Anal. calc. for $C_{50}H_{34}F_{15}NO_2P_2$ (1027.8): C 58.43, H 3.33, N 1.36; found: C 57.36, H 3.45, N 1.42.

X-Ray Crystallographic Analysis of **3a**. $C_{11}H_5F_9O_2$ (340.15 g mol^{-1}); diffractometer *IPDS-I, Stoe & Cie.* Darmstadt, Germany; Mo-K_α (graphite monochromator, λ 0.71073 Å); T 293(2) K; $2\theta_{max} = 56.30°$;

125 images, $0° \leq \varphi \leq 250°$; $\Delta\varphi = 2°$; indices: $-22 \leq h \leq 22$, $-22 \leq k \leq 22$, $-11 \leq l \leq 11$; $\rho_{calc} = 1.765$ g cm^{-3}; 29837 reflection intensities measured of which 3128 were symmetrically independent; $R_{int} = 0.0686$, $F(000) = 1344$, $\mu = 0.206$ mm^{-1}. Tetragonal, $P4_2/n$ (no. 86), $a = 17.3142(17)$, $c = 8.5421(11)$ Å, $V = 2560.8(5)$ Å^3, $Z = 8$. Structure solution and refinement were carried out with the programs SIR-92 [20] and SHELXL-97 [21]. H-Atoms were all identified in a difference *Fourier* synthesis. They were included as individual atoms with free positional and isotropic displacement parameters in the refinement. A numerical absorption correction was applied after optimization of the crystal shape (X-RED [22] and X-SHAPE [23]). R_1 and wR_2 value for 1404 reflections with $I_0 > 2\sigma(I_0)$ 0.0416 and 0.1002, and for all data 0.1075 and 0.1184; $S_{all} = 0.937$. CCDC-651118 contains the supplementary crystallographic data for this paper. These data can be obtained free of charge *via* www.ccdc.cam.ac.uk/data_request.cif from the *Cambridge Crystallographic Data Centre.*

REFERENCES

[1] G. K. S. Prakash, A. K. Yudin, *Chem. Rev.* **1997**, *97*, 757; G. G. Furin, *Russ. J. Org. Chem.* **1997**, *33*, 1209; R. P. Singh, J. M. Shreeve, *Tetrahedron* **2000**, *56*, 7613; E. Abele, E. Lukevics, *Main Group Met. Chem.* **2001**, *24*, 315.

[2] N. Maggiarosa, W. Tyrra, D. Naumann, N. V. Kirij, Y. L. Yagupolskii, *Angew. Chem.* **1999**, *111*, 2392; *Angew. Chem., Int. Ed.* **1999**, *38*, 2252.

[3] R. Krishnamurti, D. R. Bellew, G. K. S. Prakash, *J. Org. Chem.* **1991**, *56*, 984.

[4] L. A. Babadzhanova, N. V. Kirij, Y. L. Yagupolskii, W. Tyrra, D. Naumann, *Tetrahedron* **2005**, *61*, 1813.

[5] F. J. McEvoy, R. F. R. Church, E. N. Greenblatt, G. R. Allen Jr., *J. Med. Chem.* **1972**, *15*, 1111.

[6] A. Fabrycy, *Rocz. Chem.* **1960**, *34*, 1837 (CAN 55:93433); A. Fabrycy, *Rocz. Chem.* **1962**, *36*, 243 (CAN 57:75800).

[7] D. P. Becker, H. Li, D. L. Flynn, *Synth. Commun.* **1996**, *26*, 3127.

[8] U. D. G. Prabhu, K. C. Eapen, C. Tamborski, *J. Org. Chem.* **1984**, *49*, 2792.

[9] I. Krossing, I. Raabe, *Angew. Chem.* **2004**, *116*, 2116; *Angew. Chem., Int. Ed.* **2004**, *43*, 2066.

[10] T. Horaguchi, C. Tsukada, E. Hasegawa, T. Shimizu, T. Suzuki, K. Tanemura, *J. Heterocycl. Chem.* **1991**, *28*, 1261.

[11] W. Tyrra, M. M. Kremlev, D. Naumann, H. Scherer, H. Schmidt, B. Hoge, I. Pantenburg, Y. L. Yagupolskii, *Chem.–Eur. J.* **2005**, *11*, 6514.

[12] D. Naumann, M. Finke, H. Lange, W. Dukat, W. Tyrrra, *J. Fluorine Chem.* **1992**, *56*, 215.

[13] M. M. Kremlev, A. I. Mushta, W. Tyrra, D. Naumann, H. T. M. Fischer, Y. L. Yagupolskii, *J. Fluorine Chem.* **2007**, *128*, 1385.

[14] C. Tamborski, U. D. G. Prabhu, K. C. Eapen, *J. Fluorine Chem.* **1985**, *28*, 139.

[15] J. Bernstein, R. E. Davis, L. Shimoni, N.-L. Chang, *Angew. Chem.* **1995**, *107*, 2689; *Angew. Chem., Int. Ed.* **1995**, *34*, 1555.

[16] I. Ruppert, K. Schlich, W. Volbach, *Tetrahedron Lett.* **1984**, *25*, 2195.

[17] A. A. Kolomeitsev, F. U. Seifert, G.-V. Röschenthaler, *J. Fluorine Chem.* **1995**, *71*, 47.

[18] J. K. Ruff, W. J. Schlientz, *Inorg. Synth.* **1974**, *15*, 84; A. Martinsen, J. Songstad, *Acta Chem. Scand., Ser. A* **1977**, *31*, 645.

[19] D. D. Perrin, W. L. F. Armarego,'Purification of Laboratory Chemicals', 3rd edn., Pergamon Press, Oxford, 1988.

[20] A. Altomare, G. Cascarano, C. Giacovazzo, SIR-92, a Program for Crystal Structure Solution, *J. Appl. Crystallogr.* **1993**, *26*, 343.

[21] G. M. Sheldrick, SHELXL-97, Program for the Refinement of Crystal Structures, University of Göttingen, Göttingen, 1997.

[22] X-RED 1.22, Stoe Data Reduction Program (C), Stoe & Cie. GmbH, Darmstadt, 2001.

[23] X-Shape 1.06, Crystal Optimisation for Numerical Absorption Correction (C), STOE & Cie. GmbH, Darmstadt, 1999.

Received August 27, 2007